Crystal Structures of the PNA−Porphyrin Complex in the Presence and Absence of Lactose: Mapping the Conformational Changes on Lactose Binding, Interacting Surfaces, and Supramolecular Aggregations[†,‡]

Manisha Goel,[§] Rajani S. Damai,[||] Dhruv K. Sethi,[§] Kanwal J. Kaur,[§] Bhaskar G. Maiya,[||,⊥] Musti J. Swamy,[||] and Dinakar M. Salunke*[,§]

National Institute of Immunology, New Delhi 110067, India, and School of Chemistry, University of Hyderabad, Hyderabad 500046, India

Received December 14, 2004; Revised Manuscript Received February 10, 2005

ABSTRACT: The extraordinary recognition specificity of lectins for carbohydrate ligands appears to be violated as they also bind to porphyrins and other noncarbohydrate ligands. In this study, crystal structures of *meso*-tetrasulfonatophenylporphyrin (H_2TPPS) bound to peanut agglutinin (PNA) in the presence and absence of lactose were determined. The binding of H_2TPPS with PNA involved 11 molecules of H_2-TPPS in different supramolecular stacking arrangements associated with a tetramer of PNA in the crystals of the PNA−H_2TPPS binary complex as well as the PNA−H_2TPPS−lactose ternary complex. The ternary complex involved lactose binding only to two subunits of the PNA tetramer, which did not have porphyrin interacting in the vicinity of the carbohydrate-binding site. Comparison of the two structures highlighted the plasticity of the carbohydrate-binding site expressed in terms of the conformational change in lactose binding. The unusual quaternary structure of PNA, which results in exposed protein−protein interaction sites, might be responsible for the porphyrin binding. The association of porphyrin in diverse oligomeric stacking arrangements observed in the PNA−H_2TPPS complex suggested the possibility of protein−porphyrin aggregation under abnormal physiological conditions. The structures described here provide a possible native conformation of the carbohydrate-binding site of PNA in the absence of the ligand, highlight mapping of the unsaturated binding surfaces of PNA using porphyrin interactions, indicate new leads toward possible application of this lectin in photodynamic therapy, and exhibit diverse modes of porphyrin−lectin interactions with implications to porphyria, a disease that results from abnormal accumulation of porphyrins.

Aberrations due to breakdown in the specificity of molecular recognition could effectively disrupt the otherwise highly regulated cellular mechanisms. For example, autoimmune disorders—a manifestation of molecular mimicry—are directly linked to the failure of the immune system in specifically discriminating self from nonself (*1*, *2*). Similarly, many amyloid-type disorders are an outcome of the nonspecific aggregation arising from improper protein folding (*3*, *4*). The factors affecting the specificity of molecular recognition have been a focus of our investigations during the past several years (*5*−*9*). We have shown that chemically independent molecules could invoke similar physiological responses, even if they do not share the entire repertoire of structural properties while interacting with the corresponding receptors, thus exhibiting functional mimicry (*5*−*7*). Mimicry between two otherwise unrelated molecules, a porphyrin and a carbohydrate moiety, in the absence of any topological similarity between them, was also evident in the previously determined crystal structure of concanavalin A (ConA) complexed with *meso*-tetrasulfonatophenylporphyrin (H_2-TPPS) (*9*). In addition to ConA, H_2TPPS has also been shown to interact with a variety of other lectins (*10*−*14*). Recently, we reported the crystallographic analysis of the binding of H_2TPPS with jacalin (*15*), showing yet another mode of lectin−porphyrin interactions. The dissimilarity of interactions of H_2TPPS with these two lectins inspired further structural studies on binding of porphyrins with other lectins possessing diverse specificities. Crystallographic analysis of H_2TPPS−peanut lectin (PNA) interaction was thus undertaken, leading to physiological insights regarding porphyrin polymerization through protein interaction.

PNA is a nonglycosylated tetrameric lectin with a molecular mass of 110 kDa. Although it is specific for the galactopyranoside moiety at the monosaccharide level, it recognizes the T-antigenic disaccharide (Galβ1−3GalNAc) with high affinity (*16*). It is also known to bind to a variety of sugar moieties, including lactose, T-antigen, methyl-β-galactose, and *N*-acetyllactosamine, with differential affinities (*17*−*20*). T-Antigen is a chemically well-defined tumor-associated antigen, and the ability of PNA to distinguish the T-antigen from the more abundant cryptic T- and Tn-antigens

[†] This work was supported by the Department of Biotechnology, Government of India (D.M.S.), and the Department of Science and Technology, Government of India (M.J.S.).

[‡] Coordinates have been deposited in the Protein Data Bank as entries 1RIR and 1RIT.

* To whom correspondence should be addressed. E-mail: dinakar@nii.res.in. Fax: 91 11 2616 2125. Phone: 91 11 2671 7113.

[§] National Institute of Immunology.

[||] University of Hyderabad.

[⊥] Deceased March 22, 2004.

10.1021/bi047377s CCC: $30.25
Published on Web 03/25/2005

has made it a useful diagnostic tool. It is also a unique lectin because of its unusual quaternary structure (*21*). The four subunits of the tetramer are not related to each other by conventional 222 or 4-fold symmetry, although they have similar tertiary structures and possess equivalent carbohydrate-binding sites.

The porphyrin−PNA binding was investigated crystallographically by determining the crystal structures of the PNA−porphyrin−lactose ternary complex at 3.10 Å resolution and the PNA−porphyrin binary complex at 3.12 Å resolution. The porphyrins bind with partial overlap with the carbohydrate-binding site in the case of two PNA subunits and with no overlap in the case of the other two subunits. The porphyrin molecules also bind to PNA in the vicinity of the exposed subunit interacting surfaces, which arise due to the unusual quaternary structure of the lectin. The comparison of the two structures also highlights the conformational change accompanying lactose binding with PNA.

MATERIALS AND METHODS

Preparation of PNA−H_2TPPS and PNA−H_2TPPS−Lactose Complex Crystals. PNA was isolated from peanut seeds and purified by affinity chromatography as described previously (*22*). The hanging drop method was used for crystallization. PNA (30 mg/mL) and the molar equivalent of H_2TPPS (Alfa Inorganics) were co-incubated for ∼2 weeks for the PNA−H_2TPPS complex. In the case of the ternary complex, 0.1 M lactose was added to the mixture. In both the cases, the reservoir solution contained 0.4 M $(NH_4)_2SO_4$ and 0.25 M NaCl in 20 mM phosphate buffer (pH 7.2).

X-ray Diffraction Data Collection. The diffraction intensity data were collected for the PNA−H_2TPPS−lactose complex and for the PNA−H_2TPPS complex on an image plate detector (Marresearch) installed on a rotating anode X-ray source (Rigaku) operated at 40 kV and 70 mA (Cu Kα radiation). The data were processed using DENZO (*23*) and subsequently scaled using SCALEPACK (*24*). The data collection statistics for both the complexes are given in Table 1.

Structure Solution and Refinement. Molecular replacement calculations were carried out using AmoRe (*25*). A tetramer of PNA (PDB entry 2PEL) was used as a model for rotation/translation function calculation between 8 and 4 Å resolution in both cases, leading to unambiguous solutions. The models were subjected to refinement using CNS (*26*). The $F_o - F_c$ map made after rigid body refinement showed clear electron density for the porphyrin ligands. Conjugate gradient minimization and unrestrained B group refinement were carried out for both crystal structures. Water molecules were picked up using $F_o - F_c$ map with an electron density cutoff of 2.5σ. The statistics of the final refined models are given in Table 1.

Table 1: Data Collection and Refinement Statistics for the Binary (with H_2TPPS) and Ternary (with lactose and H_2TPPS) Complexes of PNA

	binary complex	ternary complex
space group	$P3_2$	$P3_2$
cell constants (Å)		
a	94.8	94.9
c	144.0	144.1
maximum resolution (Å)	3.12	3.10
completeness (%)	90.7	89.7
completeness in the last shell (%)	94.7	91.2
no. of observed reflections	58861	50192
no. of unique reflections	25840	26376
multiplicity	2.3	1.9
average $I/(\sigma I)$	7.6	7.9
average $I/(\sigma I)$ in the last shell	2.0	1.8
R_{merge} (%)	8.4	9.1
no. of solvent atoms	48	42
rms deviation for bond lengths (Å)	0.011	0.010
rms deviation for bond angles (deg)	1.51	1.47
R_{cryst} (%)	22.6	22.0
R_{free} (%)	26.3	24.5
R_{cryst} in the last shell (%)	33.6	35.9
R_{free} in the last shell (%)	38.5	39.4

RESULTS AND DISCUSSION

Overall Structures of the PNA−H_2TPPS and PNA−H_2TPPS−Lactose Complexes. PNA cocrystallizes with H_2TPPS with a symmetry packing that is different from that of any of its complexes with carbohydrate ligands determined earlier (*18*−*21*). The molecular packing of the PNA−H_2TPPS complex in crystals is shown in Figure 1. The ternary complex of PNA with H_2TPPS and lactose also crystallized with a symmetry packing similar to that observed for the binary complex. The asymmetric unit in the PNA−H_2TPPS binary complex consists of 11 H_2TPPS molecules associated with a tetramer of PNA (Figure 2a). The asymmetric unit in the ternary complex consists of two lactose molecules in addition to the 11 H_2TPPS molecules associated with a tetramer of PNA. Only two of the four subunits of PNA, therefore, show bound lactose (Figure 2b). Thus, both the quaternary structure of PNA and the arrangement of porphyrin molecules in the two complexes are identical.

The characteristic "open" quaternary structure of PNA, similar to that in the PNA−lactose complex (*17*), is preserved in both structures. The tetramer of PNA exists as a dimer of two dimers, with subunits A and D constituting a dimer associated with another dimer comprised of subunits B and C. The subunit interactions at the interface of subunits A and D are similar to those at the interface of subunits B and C. However, the subunit A and B interaction site is different from that of subunits C and D. The association of subunits A and B is similar to the expected canonical form of subunits as seen in ConA. This interface can thus be termed A−B, which is unoccupied in subunits C and D. The association mode of subunits C and D is unique to the PNA tetramer (*17*), the interaction site corresponding to the C−D interface is exposed to solvent in subunits A and B. Thus, three different intersubunit interfaces exist on each subunit. One of the interacting surfaces is involved in monomer−monomer contacts leading to the formation of the dimer. The remaining two interaction surfaces, involved in forming the tetramer from two dimers, are exposed in each of the other two subunits.

The 11 H_2TPPS molecules bound to the PNA tetramer in the asymmetric unit are distributed in five crystallographically independent clusters (Figure 2a,b). All the porphyrin molecules exhibit well-defined electron density suggesting reasonable occupancy. A pair of porphyrin molecules stacked together through $\pi-\pi$ interactions is associated with each of the four monomers. Another set of three porphyrins,

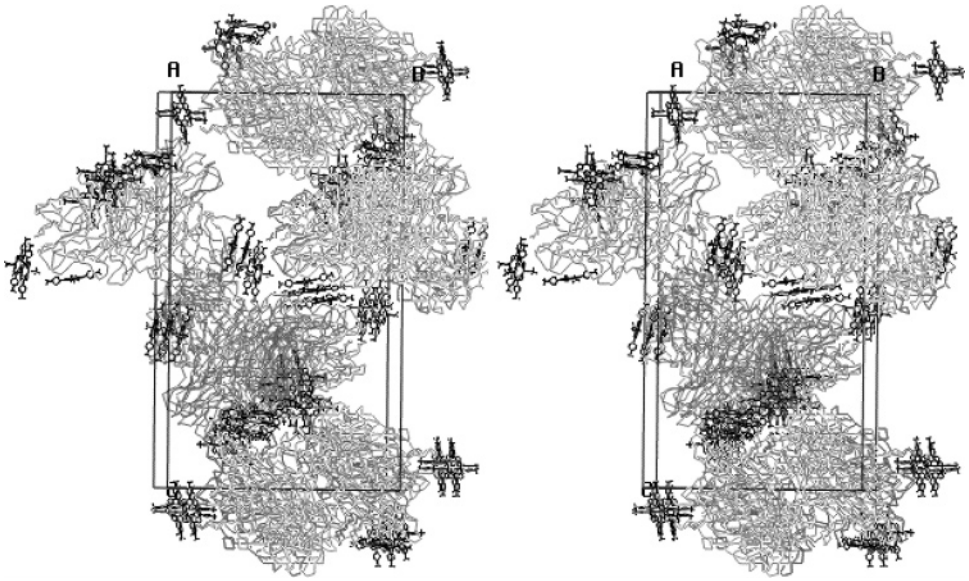

FIGURE 1: Stereo diagram of the molecular packing of the PNA−H_2TPPS complex in the crystal unit cell viewed along the crystallographic *a* axis showing cross-linking of the peanut lectin tetramer through a complex network of stacked H_2TPPS molecules.

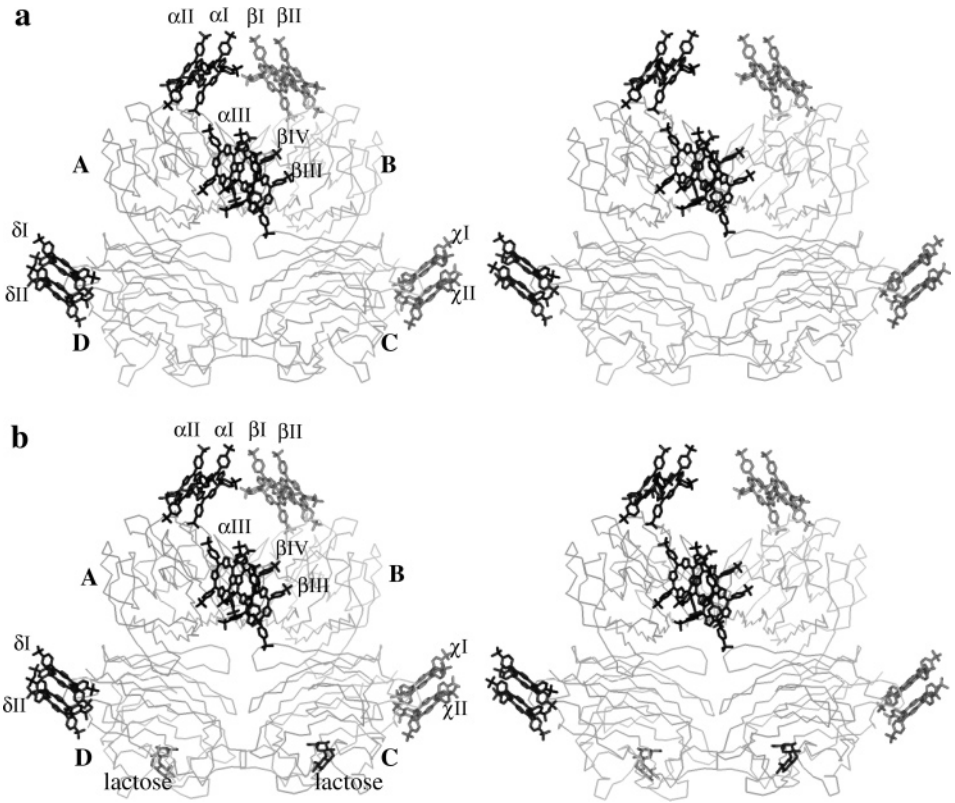

FIGURE 2: Tetramer of peanut lectin (gray) showing interactions with 11 H_2TPPS (black) molecules. Stereo drawing of the contents of the asymmetric unit of the (a) porphyrin−PNA binary complex and (b) porphyrin−PNA−lactose ternary complex in the respective crystal structures. Lactose (black) occupies the carbohydrate-binding site in subunits C and D of the PNA ternary complex but not in subunits A and B. The H_2TPPS molecules are labeled according to their association with the PNA subunits.

similarly stacked, mediates interactions of subunit A with subunit B of a symmetry-related tetramer. The porphyrin pairs associated with subunits A and B bind at equivalent positions. Similarly, the pairs of porphyrins interacting with subunits C and D are also equivalently juxtaposed. However, the interaction sites of porphyrin pairs of subunits A and C are not equivalent, nor are those of the B and D pair. Thus, effectively the stacks of porphyrins interact with PNA at three independent sites. The pair of stacked porphyrins binding at subunits A and B of one tetramer also interact with the symmetry-related D and C subunits, respectively. The pairs of stacked porphyrins associated with subunits C and D do not interact with any symmetry-related protein molecules. Instead, they interact with the porphyrin stacks associated with subunits A and B of symmetry-related tetramers, leading to the formation of a set of four porphyrins through stacking interactions. Thus, the association of porphyrins in forming a finite stack through $\pi-\pi$ interactions, while binding to different PNA subunits and the symmetry-related molecules, results in PNA−H_2TPPS cross-linking, forming an infinite

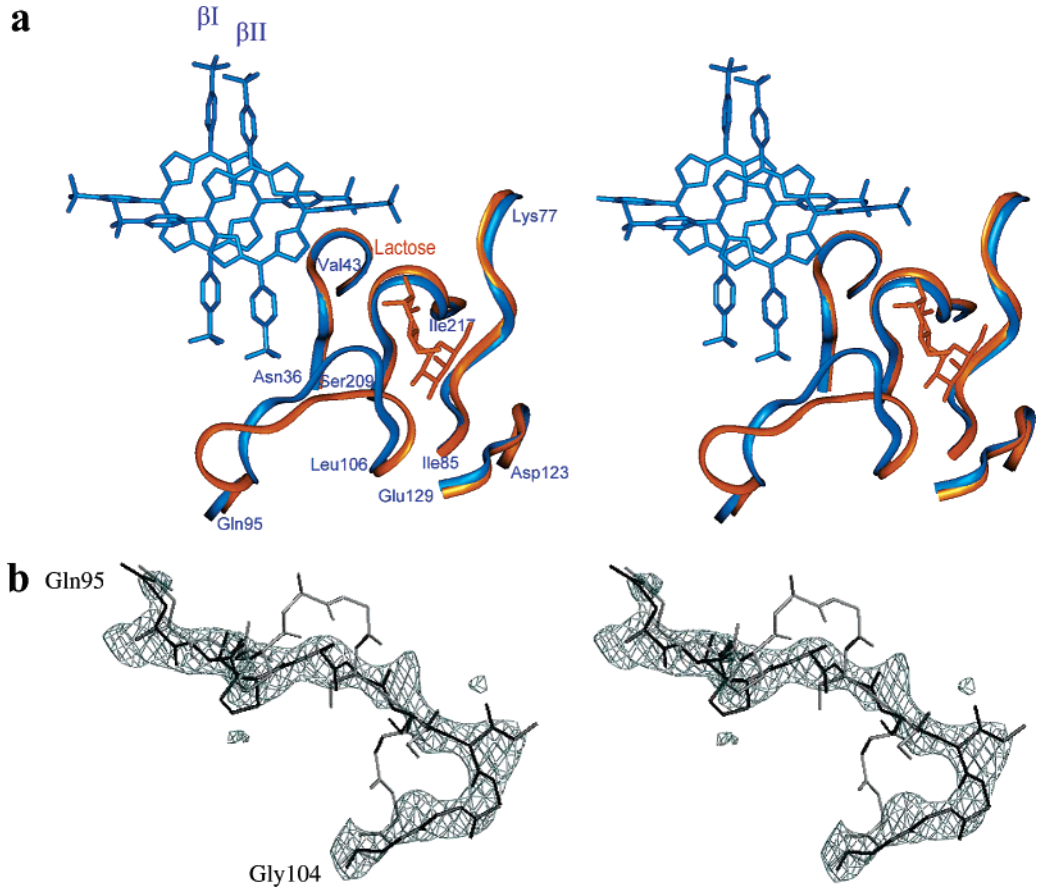

FIGURE 3: Stereoscopic images highlighting the conformational change in the carbohydrate-binding site of PNA upon lactose binding. (a) Comparison of the binding site loop conformation between subunit D of the PNA−H_2TPPS binary complex (blue) and lactose-bound subunit D of the PNA−lactose−H_2TPPS ternary complex (orange). In the ternary complex, the conformation of the PNA (ribbon) loop comprising residues 95−106 is different from that of the binary complex in lactose-bound subunits C and D (sticks) but is same as that in the binary complex for subunits A and B. (b) The $2F_o - F_c$ electron density map for the conformation of the loop comprising residues 95−104 of subunit D of the binary complex, contoured at 1.0σ. The alternate conformation of the loop, as seen in lactose-bound subunit D of the ternary complex, is superimposed in gray.

supramolecular network of lectin molecules (Figure 1).

Two of the four carbohydrate-binding sites of PNA are partially occupied by porphyrins, and the other two are completely unoccupied in the PNA−H_2TPPS binary complex. Two pairs of porphyrins interacting with subunits A and B bind near the corresponding lactose binding sites, partially covering it, while the porphyrin association in subunits C and D is farther from the carbohydrate-binding sites. In the ternary complex, lactose molecules occupy the carbohydrate-binding sites of subunits C and D, while the carbohydrate-binding sites of subunits A and B remain empty (Figure 2b).

The monomer of PNA consists of a single chain of 236 residues. Only the first 232 of the 236 residues of the PNA monomer could be traced, as the electron density for the last four residues was perhaps disordered. The tertiary structure of subunits A and B was similar in binary and ternary complexes. However, in the case of subunits C and D, the loop of residues 95−106 exhibits a different conformation in the ternary complex (with bound lactose) as compared to the binary complex (without lactose), while the rest of the structure was similar. Comparison of the carbohydrate-binding site geometries in the two structures has been elucidated in Figure 3. The rmsd for the loop involving residues 95−106 of the subunits that possess the lactose and the porphyrins bound together and that of the subunits having only the porphyrins bound is ∼3.4 Å. The largest change is observed for residue Gly102, the main chain of which is displaced toward the opening of the carbohydrate-binding cavity by ∼6.3 Å.

Structural Comparison of the Binary and Ternary Complexes Suggests Conformational Rearrangement in the Carbohydrate-Binding Site on Lactose Binding. The carbohydrate-binding site of PNA is essentially made up of four loops, residues 75−83, 91−106, 125−135, and 211−216 (*20*, *21*, *27*). The comparison of two crystal structures reported here indicates a conformational difference in the carbohydrate-binding site of PNA depending on the presence or absence of lactose. The conformation of loop 95−106 is identical within all the four subunits of the PNA−H_2TPPS complex. Interestingly, it is different from the corresponding loop in the lactose−PNA complex (*17*). The conformation of loop 95−106, for subunits A and B in the ternary complex, was the same as that in the binary complex. However, this loop adopts a conformation similar to that in the case of the lactose−PNA complex for subunits C and D. This is due to the lactose molecule occupying the carbohydrate-binding site. As mentioned above, the H_2TPPS molecules were bound away from the carbohydrate-binding site in these subunits. Thus, comparison of subunits C and D in the binary complex with the corresponding subunits in the ternary complex suggested that the loop conformation was different depending

on the presence or absence of the lactose moiety (Figure 3).

The porphyrins associated with subunits A and B exhibited an influence on the carbohydrate-binding site through the interactions with loop 95−106, which was apparently locked in the conformation corresponding to the lactose-free state in the ternary complex. This native state was stabilized in the porphyrin−PNA binary complexes due to the favorable interactions of this loop with porphyrin αII in subunit A and porphyrin *β*II in subunit B. This is consistent with the observation that the two subunits of the ternary complex (A and B), which have porphyrins interacting close to the carbohydrate-binding site, exhibit no density for the lactose moiety. On the other hand, in subunits C and D, no such interactions were observed and the lactose binding was accompanied by a conformational change as seen in the ternary complex. Thus, since the porphyrins were bound at unrelated positions in two of the four subunits of PNA, it was possible to structurally define the carbohydrate-binding site in the absence of a carbohydrate ligand. It is evident that the structure of the carbohydrate-binding site in the carbohydrate-free state is different from that in the carbohydrate-bound state. In other words, PNA undergoes a conformational change in loop 95−106 while binding to the carbohydrate ligand.

Although the conformational plasticity of the carbohydrate-binding site has been suggested in some galactose-binding lectins, it has been generally believed that the legume lectins do not exhibit conformational changes associated with carbohydrate binding (*28*). However, differential water-mediated interactions at the carbohydrate-binding site have been shown to modulate binding interactions required for recognizing different sugars by lectins (*19*). It had previously been suggested that PNA does not crystallize in the absence of a ligand (*17*−*20*). Crystal structures of PNA determined under acidic conditions, however, showed that the ligand occupancy in the case of PNA−lactose complexes was not saturated. Crystals of PNA have also been obtained in the presence of a peptide, although the peptide could not be imaged in the corresponding electron density maps. The tertiary and quaternary structures of peanut lectin were reported to be identical in all the previous studies. Since the four loops showed common conformational preferences in all the structures of PNA hitherto determined, it had been proposed that the geometry of the carbohydrate-binding site of PNA was preformed and does not undergo any substantial change on ligand binding (*21*, *27*). In the porphyrin complexes reported here, it is evident that the binding of the lactose moiety brings about a conformational change in loop 95−106. The bound water structure was also found to be simultaneously affected. Thus, our structures illustrate the role of conformational changes in the carbohydrate-binding site for mediating the degeneracy of interactions while accommodating diverse ligands by PNA.

Interactions of H_2TPPS with PNA Correlate with the "Exposed" Binding Surfaces. In addition to the carbohydrate-binding sites, the unusual quaternary structure appears to be responsible for the porphyrin association with PNA. The porphyrin pairs (αI and αII, and *β*I and *β*II) interact at equivalent positions on PNA subunits A and B; i.e., the residues of the respective subunits interacting with the two porphyrins are mostly conserved. Also, the interactions of the porphyrin pair (*χ*I and *χ*II) with subunit C were equivalent to those of porphyrins (*δ*I and *δ*II) bound to subunit D. Similarly, the interactions of porphyrin αIII with subunit A are equivalent to those of porphyrin *β*III with subunit B of a symmetry-related molecule. Porphyrin *β*IV alone does not have an equivalent. The geometrical relationships of these equivalences are evident in Figure 2. The detailed contacts of one set of porphyrins with the PNA residues are illustrated in Figure 4.

Porphyrin *β*I interacts with only four residues of subunit B and three residues of subunit C of a symmetry-related molecule (Figure 4a). Porphyrin *β*II shows van der Waals contacts with six residues of subunit B and two residues of symmetry-related subunit C. The porphine core interacts with two hydrophobic residues of subunit B, while also interacting with another hydrophobic residue of the symmetry-related molecule. Figure 4b depicts the interactions of porphyrins *δ*I and *δ*II with the residues of subunit D. Porphyrin *δ*I interacts with five residues of the protein. The oxygen atoms of the sulfonate group appear to be involved in hydrogen bonding interactions with the lectin. The porphine core does not show any interactions with the protein. Porphyrin *δ*II interacts with three residues of the subunit. The formation of stacks of four porphyrins by the interaction of the pair of porphyrins of subunit C (*χ*I and *χ*II) with that of subunit A (αI and αII) and of subunit D (*δ*I and *δ*II) with porphyrins of subunit B (*β*I and *β*II) further stabilizes this crystal packing. The interactions of porphyrins αIII, *β*IV, and *β*III with subunits A and B are depicted in Figure 4c. Among the various porphyrins associated with subunit B, porphyrin *β*III shows maximum interactions with the protein molecule with 14 residues being within van der Waals radii. Major interactions of porphyrin *β*IV are with the other two porphyrins, αIII and *β*III, between which it is sandwiched through stacking interactions, forming a trimer. Two residues from subunit B and one from subunit A lie within van der Waals distance of porphyrin *β*IV.

The unusual quaternary structure of the PNA tetramer results in three different intersubunit binding sites (*17*). One of them is vacant in two subunits, and a different one is vacant in the other two subunits. The C−D interaction site associating the C and D subunits is free in subunits A and B; this site is occupied in the porphyrin−PNA structure by the αIII and *β*III porphyrins. Approximately 14 residues of PNA subunit A are involved in van der Waals contacts with porphyrin αIII, and nine of these residues are the same as those involved in the intersubunit interactions in subunits C and D. Thus, porphyrin αIII presumably binds to this site because of the exposed features. The other site, involved in the interaction of subunits A and B, is free in subunits C and D. Two residues from this site on subunit C interact with the porphyrin dimer, *χ*I and *χ*II. One of these residues, Arg53, interacts with the sulfonate oxygens of H_2TPPS. Arg53 has previously been shown to be involved in mediating the hydrogen bonding interactions even while participating in intersubunit associations (*17*).

The porphyrin association with PNA is thus facilitated by the interaction with the exposed intersubunit contact sites (αIII, *β*III, and *β*IV) (Figure 5a). Interactions with the hydrophobic residues near the carbohydrate-binding site may represent the binding of porphyrins (αI, αII, *β*I, and *β*II), at the extended carbohydrate-binding site (Figure 5b) as seen in the case of peptide binding to ConA (*6*). Physiologically,

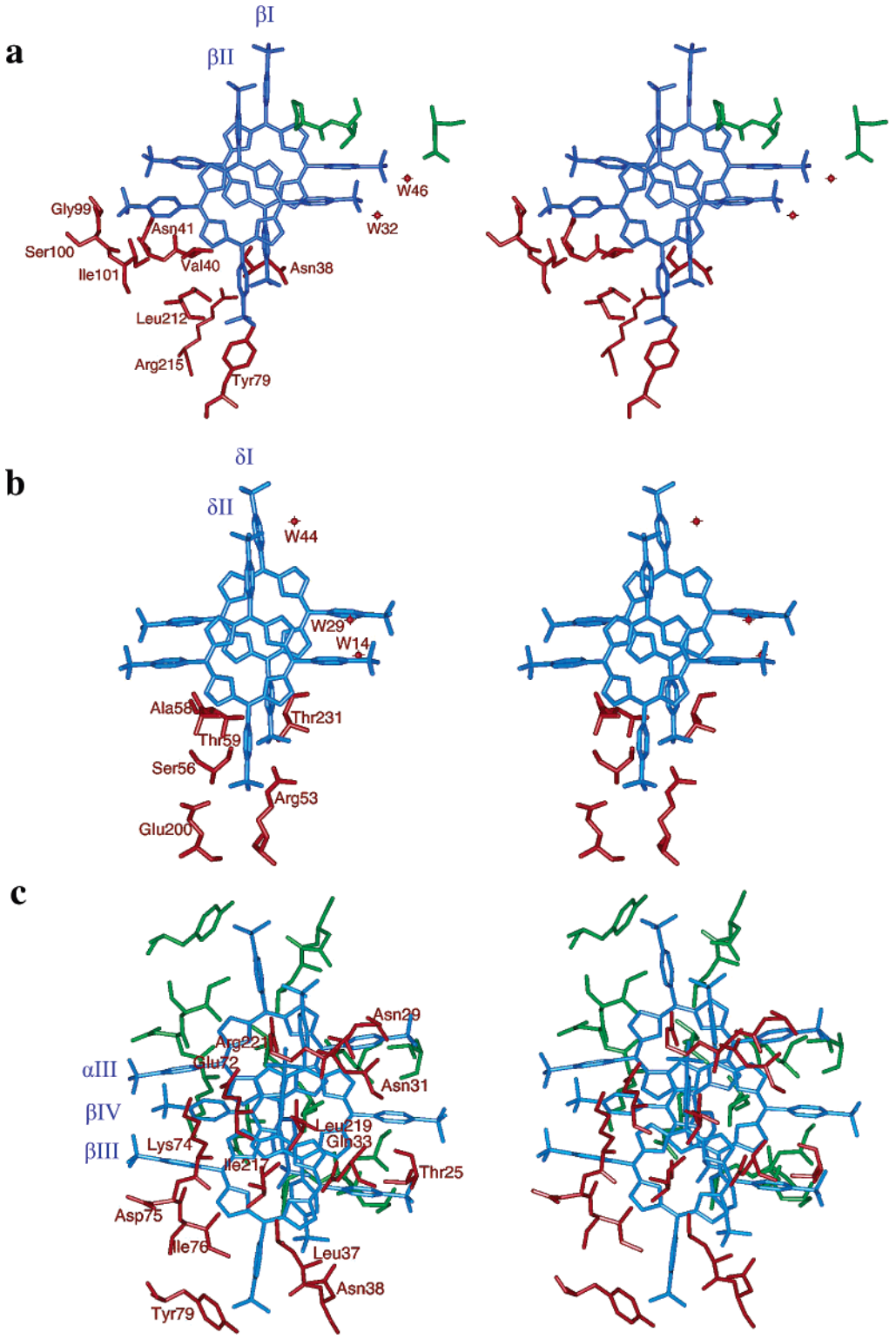

FIGURE 4: Stereoscopic drawings showing stacked oligomers of H_2TPPS exhibiting interactions with PNA in three independent modes in the binary and ternary complex of PNA with porphyrin and lactose. (a) Interactions of the pair of porphyrins, βI and βII (blue), with the residues of subunit B (red) and symmetry-related subunit C (green) of PNA. (b) Interactions of porphyrins δI and δII (blue) at the porphyrin-binding site of subunit D (red) of PNA. (c) Association of a trimer of porphyrins, βIII, βIV, and αIII (blue), with PNA subunit B (red) and subunit A (green) in a symmetrical manner. Residues of the symmetrically related subunit have not been labeled to avoid cluttering.

the carbohydrate moieties binding to the lectins are large complex carbohydrates on the cell surface. The natural ligand binding site of lectins is thus expected to be larger in surface area than that mapped from the crystallographic analyses involving small sugars. Therefore, even with the narrow overlap of the porphyrin binding site with respect to the lactose binding site, as in subunits A and B, it may still be part of the binding site for the natural carbohydrate ligand (*6*). Porphyrin pairs χI and χII and δI and δII interact through hydrogen bonding with subunits C and D, respectively (Figure 5c). This porphyrin interaction site is close to the A−B subunit interaction site, with two residues being

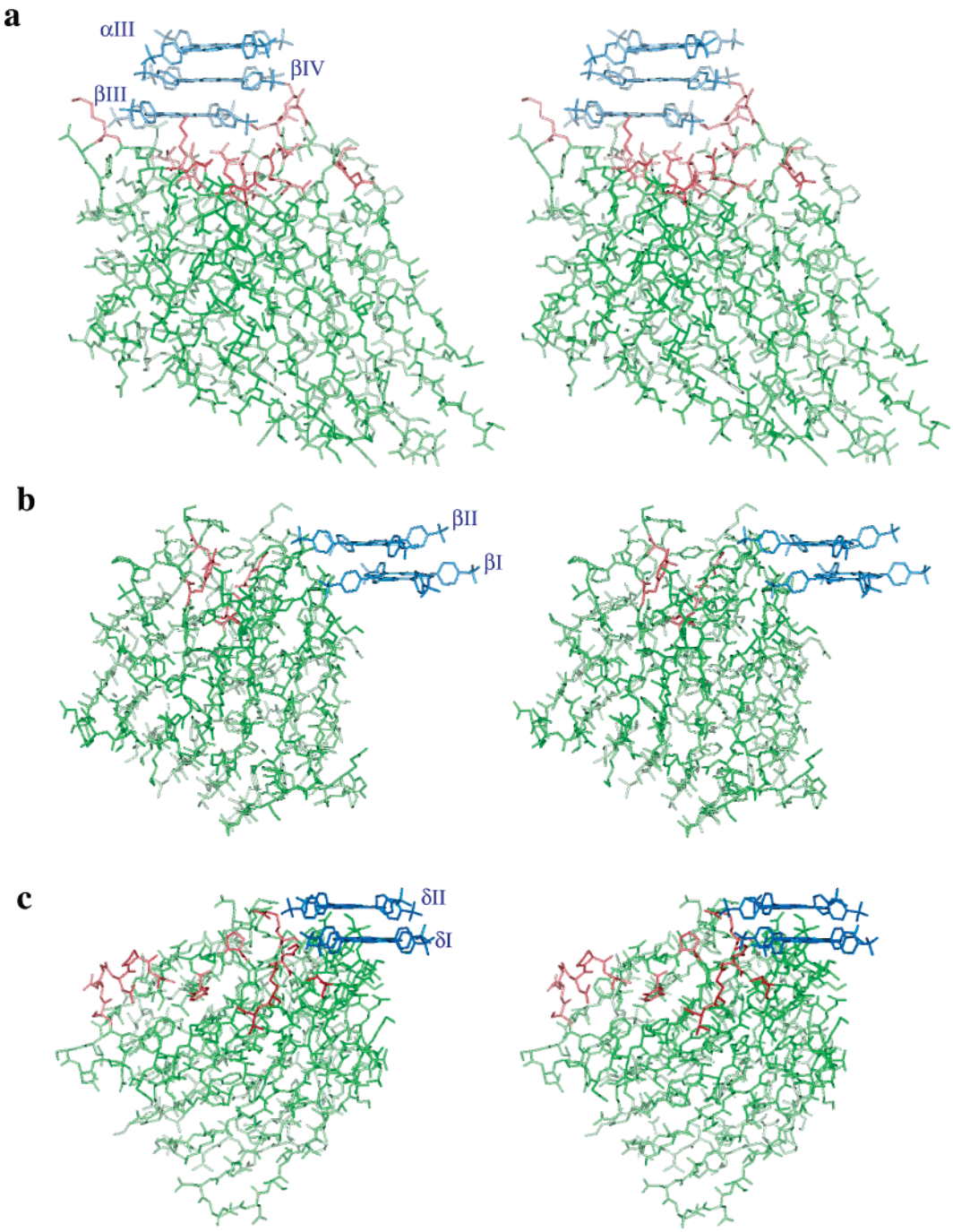

FIGURE 5: Porphyrin association with the three "interacting" sites of PNA. (a) Stereo drawing showing the binding of porphyrins βIII, βIV, and αIII on subunit B at the site corresponding to the C−D interface. The residues involved in the C−D interface in subunit B are highlighted in red. (b) Stereo drawing showing the binding of porphyrins βI and βII, with a narrow overlap at the lactose binding site, on subunit B. Residues involved in lactose binding are colored red. (c) Stereo drawing showing the binding of porphyrins δI and δII to subunit D at a site corresponding to the A−B subunit interface. The residues involved in the A−B interface in subunit D are highlighted in red.

involved in both interactions. Thus, the exposed interaction sites arising from the unusual quaternary structure are also used as attachment points for the porphyrin molecules.

The binding of porphyrin to PNA at the sites outside the carbohydrate-binding sites in at least two subunits is of considerable interest in photodynamic therapy, a relatively new approach for the treatment of malignant tumors (*29*). Because of its specific recognition of the tumor-specific Thomsen−Friedenreich antigen (*16*), PNA is a suitable candidate for targeting porphyrins to tumor cells. As is evident from the ternary complex, the porphyrin binding does not preclude its ability to bind to the carbohydrate antigen, and therefore, the targeting by PNA is feasible. Indeed, the structures of the PNA−porphyrin complex and the PNA−lactose−porphyrin complex provide interesting new leads for suggesting possible applications of this lectin in photodynamic therapy.

Comparison of Porphyrin Interaction with PNA, Con A, and Jacalin: Physiologically Relevant Supramolecular Aggregation. Comparison of the complexes of H_2TPPS with PNA and two other lectins, ConA and jacalin, which have been previously analyzed (*9*, *15*), provided insights with regard to lectin−porphyrin binding. An attractive invariant feature among the three lectin−H_2TPPS complexes in

crystals was the supramolecular association of the porphyrin along with the lectin even though the molecular interactions involving different lectins and H_2TPPS are very different. A finite set of stacked porphyrin molecules interact through $\pi-\pi$ interactions between themselves while cross-linking the multivalent lectin molecules. Besides, the porphyrin pairs also interact with the corresponding symmetry-related pairs forming stacks of four porphyrins in this case. In the complex with ConA, the porphyrins interact with the crystallographically related lectin subunits in a symmetrical manner. On the other hand, the two porphyrins of the stack interact at two different sites on jacalin. While the stacks of porphyrin pairs interact with PNA subunits in two different modes, the stack of three porphyrins mediated interaction between subunits A and B in a symmetrical manner. The H_2TPPS molecules constituting the stacks are arranged in a variety of fashions. The two porphyrins of the different stacked pairs are translated with respect to each other, whereas the porphyrins, which are part of the stack of three molecules, are arranged in a fanlike manner. The stereoscopic images of different stacking arrangements with respect to their protein environment in PNA−H_2TPPS crystals are illustrated in Figure 4. Two porphyrins of the stack in the ConA−H_2-TPPS structure are staggered with respect to each other such that their porphine cores are rotated. This mode of stacking has also been seen in porphyrin complexed with calixarene supramolecular assemblies (*30*) and in other metalloporphyrin dimers (*31*). The mode of stacking of the two porphyrins in the jacalin−porphyrin complex resembles that in the case of PNA−porphyrin pairs. The different modes of porphyrin stacking and the associated energetics have been extensively modeled (*32*). The observed variety of modes in which porphyrin dimers show $\pi-\pi$ association while binding to lectins is consistent with the possibilities predicted from energy considerations.

The two crystal structures of H_2TPPS complexed with PNA presented here are different from those with ConA and jacalin reported previously (*9*, *15*), possibly due to the unusual quaternary structure of PNA. However, the formation of infinite three-dimensional arrays involving multivalent carbohydrate-binding proteins and porphyrins, as seen in their crystals, appears to be a common property of all three otherwise unrelated lectin−porphyrin complexes. Porphyrins also exhibit inherent self-assembly properties through $\pi-\pi$ stacking in diverse modes forming finite-sized oligomers. The potential for self-assembly and for binding to the carbohydrate-binding surfaces of porphyrins together may be responsible for the porphyrin−lectin polymer formation in crystals. It is possible that such polymers could exist under saturating conditions in solution as well.

The supramolecular aggregation observed in crystals may actually relate to the molecular pathology of porphyria, a disorder caused by genetic alterations in the enzymatic pathway involved in heme biosynthesis (*33*, *34*). Breakdown in the heme biosynthesis machinery results in the excessive accumulation of the porphyrin precursors leading to the deposition of porphyrins in blood, skin, and neuronal tissues (*35*, *36*). One of the consequences of this disorder, resulting from the photochemical properties of porphyrins, is skin photosensitivity. More serious consequences such as neuropsychiatric symptoms could also result (*35*, *37*). On the basis of our results, it is attractive to hypothesize that the supramolecular cross-linking involving lectin-like molecules and the multipotently reactive porphyrin molecules observed in the crystal structures may result in supramolecular polymerization in vivo. This polymerization, in turn, may lead to impairment of cellular functions, akin to the cellular dysfunctioning that has been associated with amyloid formation in some of the other neurodegenerative disorders. Our hypothesis draws strength from the observation that the practiced therapies for acute porphyria include a carbohydrate rich diet and administration of glucose (*38*, *39*). Consistent with the carbohydrate therapy for porphyria, competition by carbohydrates with the porphyrins in the aggregates could facilitate dissolution of the aggregates formed through the association of porphyrins and the lectin-like multivalent carbohydrate binding proteins.

CONCLUSIONS

Thus, the comparison of the crystal structures of PNA complexed with H_2TPPS, in the presence as well as absence of lactose, indicated conformational changes in the carbohydrate-binding sites with respect to ligand binding. We suggest that the unliganded subunits in both our structures represent the native conformation of the PNA molecule. Comparison of the structure of lactose-free subunits with the corresponding structure of lactose-bound subunits of the ternary complex implies that the conformational change in this loop may be a prerequisite for carbohydrate ligand binding.

Additionally, the analysis of the binding of the unusually large number of porphyrin molecules to PNA provided remarkable insights with regard to the ligand recognition mechanisms involving PNA. Interactions of porphyrin with PNA can be correlated with the exposed binding surfaces resulting from the unusual quaternary structure. The unusual quaternary structure of peanut lectin is responsible for generating adhesive regions where multipotent porphyrin molecules could bind.

The porphyrins associated with different subunits of PNA stack in three different modes. In addition to the porphyrin association in the vicinity of the carbohydrate-binding sites, the diverse stacking modes of porphyrin also facilitated the stability of the lectin−porphyrin complex in crystals. The most invariant feature of these crystal structures was the self-association of the porphyrin molecules to form stacked pairs through diverse interactions cross-linking the lectin molecules. It is attractive to hypothesize that the accumulating porphyrins in diseases such as porphyria aggregate through lectin-like proteins in a variety of nonspecific supramolecular assemblies leading to cellular dysfunction.

REFERENCES

1. del Guercio, P. (1993) The self and the nonself: Immunorecognition and immunologic functions, *Immunol Res. 12*, 168−182.
2. Sinha, A. A., Lopez, M. T., and McDevitt, H. O. (1990) Autoimmune diseases: The failure of self-tolerance, *Science 248*, 1380−1388.
3. Aguzzi, A., and Haass, C. (2003) Games played by rogue proteins in prion disorders and Alzheimer's disease, *Science 302*, 814−818.
4. Stefani, M., and Dobson, C. M. (2003) Protein aggregation and aggregate toxicity: New insights into protein folding, misfolding diseases and biological evolution, *J. Mol. Med. 81*, 678−699.

5. Kaur, K. J., Khurana, S., and Salunke, D. M. (1997) Topological analysis of the functional mimicry between a peptide and a carbohydrate moiety, *J. Biol. Chem. 272*, 5539−5543.
6. Jain, D., Kaur, K. J., Sundaravadivel, B., and Salunke, D. M. (2000) Structural and functional consequences of peptide-carbohydrate mimicry. Crystal structure of a carbohydrate-mimicking peptide bound to concanavalin A, *J. Biol. Chem. 275*, 16098−16102.
7. Jain, D., Kaur, K. J., Goel, M., and Salunke, D. M. (2000) Structural basis of functional mimicry between carbohydrate and peptide ligands of Con A, *Biochem. Biophys. Res. Commun. 272*, 843−849.
8. Kaur, K. J., Jain, D., Goel, M., and Salunke, D. M. (2001) Immunological implications of structural mimicry between a dodecapeptide and a carbohydrate moiety, *Vaccine 19*, 3124−3130.
9. Goel, M., Jain, D., Kaur, K. J., Kenoth, R., Maiya, B. G., Swamy, M. J., and Salunke, D. M. (2001) Functional equality in the absence of structural similarity: An added dimension to molecular mimicry, *J. Biol. Chem. 276*, 39277−39281.
10. Bhanu, K., Komath, S. S., Maiya, B. G., and Swamy, M. J. (1997) Interaction of porphyrin with concanavalin A and pea lectin, *Curr. Sci. 73*, 598−602.
11. Kenoth, R., Reddy, D. R., Maiya, B. G., and Swamy, M. J. (2001) Thermodynamic and kinetic analysis of porphyrin binding to *Trichosanthes cucumerina* seed lectin, *Eur. J. Biochem. 268*, 5541−5549.
12. Komath, S. S., Kenoth, R., Giribabu, L., Maiya, B. G., and Swamy, M. J. (2000) Fluorescence and absorption spectroscopic studies on the interaction of porphyrins with snake gourd (*Trichosanthes anguina*) seed lectin, *J. Photochem. Photobiol., B 55*, 49−55.
13. Komath, S. S., Bhanu, K., Maiya, B. G., and Swamy, M. J. (2000) Binding of porphyrins by the tumor-specific lectin, jacalin [Jack fruit (*Artocarpus integrifolia*) agglutinin], *Biosci. Rep. 20*, 265−276.
14. Sultan, N. A. M., Maiya, B. G., and Swamy, M. J. (2004) Thermodynamic analysis of porphyrin binding to *Momordica charantia* (bitter gourd) lectin, *Eur. J. Biochem. 271*, 3274−3282.
15. Goel, M., Anuradha, P., Kaur, K. J., Maiya, B. G., Swamy, M. J., and Salunke, D. M. (2004) Porphyrin binding to jacalin is facilitated by the inherent plasticity of the carbohydrate-binding site: Novel mode of lectin-ligand interaction, *Acta Crystallogr. D60*, 281−288.
16. Swamy, M. J., Gupta, D., Mahanta, S. K., and Surolia, A. (1991) Further characterization of the saccharide specificity of peanut (*Arachis hypogaea*) agglutinin, *Carbohydr. Res. 213*, 59−67.
17. Banerjee, R., Das, K., Ravishankar, R., Suguna, K., Surolia, A., and Vijayan, M. (1996) Conformation, protein-carbohydrate interactions and a novel subunit association in the refined structure of peanut lectin-lactose complex, *J. Mol. Biol. 259*, 281−296.
18. Ravishankar, R., Ravindran, M., Saguna, K., Surolia, A., and Vijayan, M. (1997) Crystal structure of the peanut lectin-T-antigen complex. Carbohydrate specificity generated by water bridges, *Curr. Sci. 72*, 855−861.
19. Ravishankar, R., Suguna, K., Surolia, A., and Vijayan, M. (1999) Structures of the complexes of peanut lectin with methyl-β-galactose and *N*-acetyllactosamine and a comparative study of carbohydrate binding in Gal/GalNAc-specific legume lectins, *Acta Crystallogr. D55*, 1375−1382.
20. Ravishankar, R., Thomas, C. J., Suguna, K., Surolia, A., and Vijayan, M. (2001) Crystal structures of the peanut lectin-lactose complex at acidic pH: Retention of unusual quaternary structure, empty and carbohydrate bound combining sites, molecular mimicry and crystal packing directed by interactions at the combining site, *Proteins 43*, 260−270.
21. Banerjee, R., Mande, S. C., Ganesh, V., Das, K., Dhanaraj, V., Mahanta, S. K., Suguna, K., Surolia, A., and Vijayan, M. (1994) Crystal structure of peanut lectin, a protein with an unusual quaternary structure, *Proc. Natl. Acad. Sci. U.S.A. 91*, 227−231.
22. Fish, W. W., Hamlin, L. M., and Miller, R. L. (1978) The macromolecular properties of peanut agglutinin, *Arch. Biochem. Biophys. 190*, 693−698.
23. Otwinowski, Z. (1993) in *Proceedings of the CCP4 Study Weekend. Data Collection and Processing* (Sawyer, L., Isaacs, N., and Bailey, S., Eds.) pp 56−62, Daresbury Laboratory, Warrington, U.K.
24. Otwinowski, Z., and Minor, W. (1997) Processing of X-ray Diffraction Data Collected in Oscillation Mode, in *Methods in Enzymology* (Carter, C. W., Jr., and Sweet, R. M., Eds.) Vol. 276, pp 307−326, Academic Press, New York.
25. Navaza, J. (1994) AmoRe: An automated package for molecular replacement, *Acta Crystallogr. A50*, 157−163.
26. Bruenger, A. T., Adams, P. D., Clore, G. M., DeLano, W. L., Gros, P., Grosse-Kunstleve, R. W., Jiang, J. S., Kuszewski, J., Nilges, M., Pannu, N. S., Read, R. J., Rice, L. M., Simonson, T., and Warren, G. L. (1998) Crystallography and NMR system: A new software suite for macromolecular structure determination, *Acta Crystallogr. D54*, 905−921.
27. Kundhavai Natchiar, S. K., Arockia, S., Jeyaprakash, A., Ramya, T. N., Thomas, C. J., Suguna, K., Surolia, A., and Vijayan, M. (2004) Structural plasticity of peanut lectin: An X-ray analysis involving variation in pH, ligand binding and crystal structure, *Acta Crystallogr. D60*, 211−219.
28. Swaminathan, C. P., Gupta, A., Surolia, N., and Surolia, A. (2000) Plasticity in the primary binding site of galactose/*N*-acetylgalactosamine-specific lectins. Implication of the C−H···O hydrogen bond at the specificity-determining C-4 locus of the saccharide in 4-methoxygalactose recognition by jacalin and winged bean (basic) agglutinin I, *J. Biol. Chem. 275*, 28483−28487.
29. Sibata, C. H., Colussi, V. C., Oleinick, N. L., and Kinsella, T. J. (2001) Photodynamic therapy in oncology, *Expert Opin. Pharmacother. 2*, 917−927.
30. Costanzo, L. D., Geremia, S., Randaccio, L., Purrello, R., Lauceri, R., Sciotto, D., Gulino, F. G., and Pavone, V. (2001) Calixarene-porphyrin supramolecular complexes: pH-tuning of complex stoichiometry, *Angew. Chem., Int. Ed. 40*, 4245−4247.
31. Song, H., Reed, C. A., and Scheidt, W. R. (1989) Dimerization of metalloporphyrin π-cation radicals: $[Zn(OEP)(OH_2)]_2(ClO_4)_2$, a novel dimer, *J. Am. Chem. Soc. 111*, 6867−6868.
32. Hunter, C. A., and Sanders, J. K. M. (1990) The nature of $\pi-\pi$ interactions, *J. Am. Chem. Soc. 112*, 5525−5534.
33. Solinas, C., and Vajda, F. J. (2004) Epilepsy and porphyria: New perspectives, *J. Clin. Neurosci. 11*, 356−361.
34. Brownlie, P. D., Lambert, R., Louie, G. V., Jordan, P. M., Blundell, T. L., Warren, M. J., Cooper, J. B., and Wood, S. P. (1994) The three-dimensional structures of mutants of porphobilinogen deaminase: Toward an understanding of the structural basis of acute intermittent porphyria, *Protein Sci. 3*, 1644−1650.
35. Utz, N., Kinkel, B., Hedde, J., and Bewermeyer, H. (2001) MR imaging of acute intermittent porphyria mimicking reversible posterior leukoencephalopathy syndrome, *Neuroradiology 43*, 1059−1062.
36. Bylesjo, I., Brekke, O. L., Prytz, J., Skjeflo, T., and Salvesen, R. (2004) Brain magnetic resonance imaging white-matter lesions and cerebraspinal fluid findings in patients with acute intermittent porphyria, *Eur. Neurol. 51*, 1−5.
37. Thunell, S. (2000) Porphyrins, porphyrin metabolism and porphyrias. I. Update, *Scand. J. Clin. Lab. Invest. 60*, 509−540.
38. Moore, M. R., and McColl, K. E. (1989) Therapy of the acute porphyrias, *Clin. Biochem. 22*, 181−188.
39. Bonkowsky, H. L., Magnussen, C. R., Collins, A. R., Doherty, J. M., Hess, R. A., and Tschudy, D. P. (1976) Comparative effects of glycerol and dextrose on porphyrin precursor excretion in acute intermittent porphyria, *Metabolism 25*, 405−414.

BI047377S